Article

Reduction of Ferric Chloride in Yeast Growth Media, by Sugars and Aluminum

Kęstutis Mažeika [1,*] , **Vytautas Melvydas** [2] **and Dovilė Čepukoit** [3]

1   Center for Physical Sciences and Technology, Savanoriu 231, LT-02300 Vilnius, Lithuania
2   Independent Researcher, LT-05128 Vilnius, Lithuania; anabaras66@gmail.com
3   Nature Research Center, Akademijos 2, LT-08412 Vilnius, Lithuania; dovile.cepukoit@gamtc.lt
*   Correspondence: kestutis.mazeika@ftmc.lt

Abstract: Iron compounds can be used in antimicrobial applications by exploiting the toxicity of divalent iron to living organisms due to the Fenton reaction. In this study, the growth inhibitory effects of ferrous sulfate $FeSO_4 \cdot 7H_2O$ and ferric chloride $FeCl_3 \cdot 6H_2O$ were observed on *Metschnikowia* clade and *Saccharomyces cerevisiae* yeast cells. The relatively high amount of reduced Fe^{3+} to Fe^{2+} in the growth medium determined by Mössbauer spectroscopy may contribute to the antimicrobial activity of ferric chloride. In order to test the reducing ability of sugars in the growth media of yeasts, the reaction of ferric chloride $FeCl_3 \cdot 6H_2O$ with sugars was investigated. In mixtures of $FeCl_3 \cdot 6H_2O$ and fructose, approximately two thirds of Fe^{3+} can be reduced to Fe^{2+}. When the mixture of $FeCl_3 \cdot 6H_2O$ and fructose is placed on the surface of aluminum foil, an iron film is formed on the surface of the aluminum due to the reduction by both fructose and aluminum. The relative amount of Fe^{3+} which was reduced to Fe^0 reached 68%.

Keywords: iron reduction; ferric chloride; *Metschnikowia* yeast; Mössbauer spectroscopy

1. Introduction

Metal oxidation and reduction take place in biological cells, in their medium, in the environment and elsewhere. In industry, obtaining pure metals from metal compounds with non-metals requires metal reduction, which is achieved using carbon, carbon monoxide, hydrogen and metallothermic reduction applying reactive metals, aqueous or molten salt electrolysis [1,2]. Many compounds can be used as reducing agents depending on the purpose. When investigating the interaction of *Metschnikowia* clade yeasts with iron in their environment [3,4], it was found that the reduced iron form, Fe^{2+}, appears both in the growth media and in yeast biomass. Since divalent iron can have toxic or inhibitory effects on yeast cells [5,6], it is important to determine the ability of compounds in growth media to reduce Fe^{3+}. Although many nutrients, including glucose or fructose, are added to the growth media, sugars have previously been reported to be mild reductants of iron [7,8].

Yeasts of the *Metschnikowia* clade are used in winemaking (together with *Saccharomyces cerevisiae*) [9] and in other biotechnological processes such as oil production [10], and their promising biocidal properties are also widely studied [11–16]. *Metschnikowia* spp. are characterized by the production of pulcherriminic acid, which binds with iron in the environment to form the red pigment pulcherrimin [17]. Some bacteria such as *Bacillus suptilis* are also characterized by pulcherrimin synthesis [18]. It was found that the amount of iron in the environment of pulcherriminic-acid-producing yeast and bacteria is regulated with the help of pulcherrimin, thus avoiding oxidative stress [5,6,16,18].

Ferric chloride is widely used as a mild oxidant or etchant, in organic polymerization reactions, in water treatment as a flocculant and coagulant and in many other reactions as a precursor and catalyst [19–24]. Ferric chloride can also be used as an oxidizer of glucose [25].

Due to the growing resistance of pathogenic microorganisms to antibiotics, the biocidal properties of various inorganic materials, including iron-containing ones such as ferritic nanoparticles and iron salts (ferrous sulfate and ferric chloride), are being studied [26–29]. In experiments with *Metschnikowia* yeast, ferric chloride was used mainly as an iron source in growth media [3,4]. In this study, the growth inhibition effects of ferric chloride $FeCl_3 \cdot 6H_2O$ and ferrous sulfate $FeSO_4 \cdot 7H_2O$ on *Metschnikowia* clade yeasts which produce pulcherrimin-immobilizing excess iron were observed. *Saccharomyces cerevisiae*, which has many domesticated strains and has a well-explored genome and is a widely used model yeast [30,31], was applied in this study to compare the antimicrobial effects of iron compounds as pulcherrimin non-synthesizing yeast. The interaction of ferric chloride ($FeCl_3 \cdot 6H_2O$) with sugars was investigated to determine the ability of sugars to reduce iron in ambient conditions. It was also found that when placing the mixture of fructose with $FeCl_3 \cdot 6H_2O$ on the aluminum foil, Fe^{3+} is reduced to the metallic state. Aluminum was used as an additional reducing agent. It can be noted that iron reduction to the metallic state has previously been observed in iron–aluminum chloride melts, but at significantly higher temperatures than ambient [32]. In another study [33], the growth inhibition of *Metschnikowia* yeast was also observed during the decomposition of metallic iron in the growth medium.

2. Results

Ferrous sulfate $FeSO_4 \cdot 7H_2O$ applied to the growth medium significantly inhibited the growth of *Metschnikowia* yeasts inoculated as streaks (Figure 1a–c). Yeast inhibition is also visible in the center of the area with brown precipitates formed at the sites of the application of ferric chloride $FeCl_3 \cdot 6H_2O$. Over time, the yeast biomass became redder, indicating the formation of a red pigment—pulcherrimin—inside the yeast biomass. Growth inhibition and red pigmentation were also observed when $FeSO_4 \cdot 7H_2O$ and $FeCl_3 \cdot 6H_2O$ were applied to the *Metschnikowia shanxiensis* M10 strain yeast lawn (Figure 1d). The inhibitory effects of ferrous sulfate $FeSO_4 \cdot 7H_2O$ and ferric chloride $FeCl_3 \cdot 6H_2O$ on the *Saccharomyces cerevisiae* lawn are shown in Figure 2a. Ferric chloride $FeCl_3 \cdot 6H_2O$ also produces brown precipitates (Figures 1 and 2a), but at the edges the inhibitory effects are similar to those of $FeSO_4 \cdot 7H_2O$. The results for four *Metschnikowia* clade yeast strains, *M. sinensis* M4 and *M. pulcherrima* MP strains exposed to $FeCl_3 \cdot 6H_2O$ and *M. sinensis* M6, *M. shanxiensis* M10 exposed to $FeSO_4 \cdot 7H_2O$, and repeated experiments with substitution of strains show little strain dependence for the inhibitory effect. With ferrous sulfate $FeSO_4 \cdot 7H_2O$, the effect is more widely distributed, which is probably due to an easier diffusion of Fe^{2+}, as in the case of $FeCl_3 \cdot 6H_2O$, where insoluble precipitates fall out.

The inhibition zone in Figure 2b is delimited by a red pigment rim around the inoculated *Metschnikowia sinensis* M4 spots and streaks indicating the active formation of insoluble pulcherrimin that binds incoming iron from the surrounding growth medium containing 5 mg/L of elemental iron. No inhibition effect in the lawn is produced by *S. cerevisiae* streaks, which do not produce pulcherriminic acid. In response to the higher iron concentration when additional ferric chloride (in solution) is applied (Figure 2b), increased red pigmentation reflects increased secretion of pulcherriminic acid. In this way, the inhibition of the *S. cerevisiae* lawn observed here is not due to the effect of Fe compounds, but due to competition with *Metschnikowia* yeasts for iron [12] when the amounts of applied iron compounds are much lower than in Figure 1.

The presence of Fe^{2+} in the growth medium after supplementing the medium with ferric chloride $FeCl_3 \cdot 6H_2O$ was observed previously [3]. In this study, in order to exclude the influence of yeasts, experiments with growth media without inoculated yeasts were performed. Upon supplementing the yeast growth media with ferrous sulfate $FeSO_4 \cdot 7H_2O$ and ferric chloride $FeCl_3 \cdot 6H_2O$, changes in the valency of iron were observed, with both Fe^{3+} and Fe^{2+} detected in the Mössbauer spectra (Figure 3). In the case of $FeSO_4 \cdot 7H_2O$, one-third of the iron ions in the dried growth medium were found in the oxidized Fe^{3+}

state, while the remainder remained Fe^{2+} (Table 1). With $FeCl_3 \cdot 6H_2O$, about a quarter of the iron in the growth medium was reduced to Fe^{2+}.
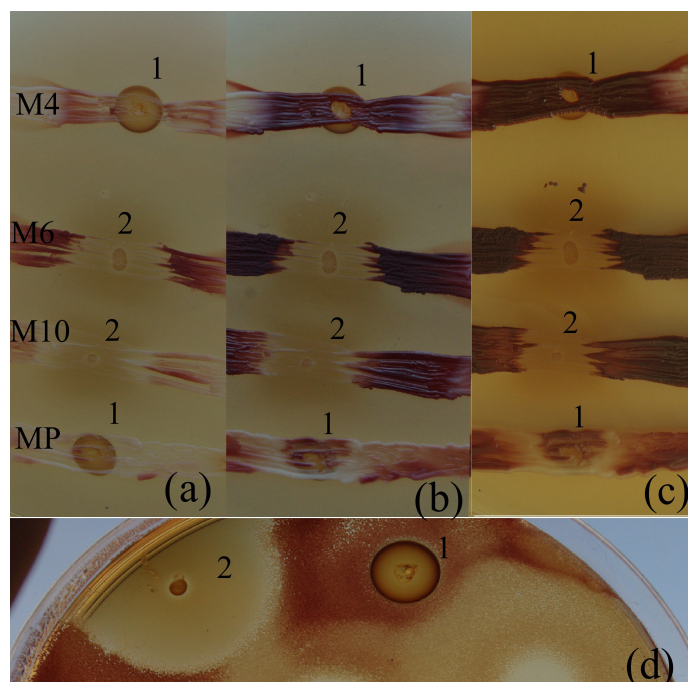
Figure 1. Effects of ferric chloride $FeCl_3 \cdot 6H_2O$ and ferrous sulfate $FeSO_4 \cdot 7H_2O$ on *Metschnikowia* spp. yeast after (**a**) 1.5 days, (**b**) 3 days and (**c**,**d**) 5 days. Yeast grown at 20 °C: (**a**–**c**) *M. sinensis* M4, M6, *M. shanxiensis* M10 and *M. pulcherrima* MP yeast biomass streaks; (**d**) M10 lawn on MR growth medium containing 1.1 mg/L of elemental Fe. At indicated places: 1—1–2 mg of $FeCl_3 \cdot 6H_2O$, 2—1–2 mg of $FeSO_4 \cdot 7H_2O$ applied 2 h after yeast inoculation.
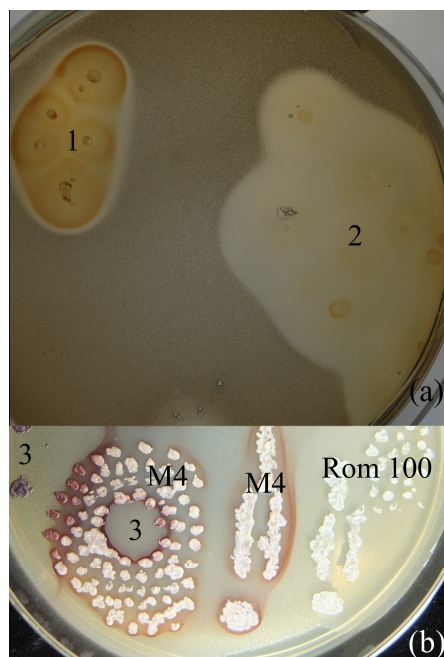
Figure 2. Effects of ferric chloride $FeCl_3 \cdot 6H_2O$ and ferrous sulfate $FeSO_4 \cdot 7H_2O$ after 5 days (**a**) and *M. sinensis* M4 and *S. cerevisiae* Rom 100 spots after 3 days (**b**) on *S. cerevisiae* lawn. MR growth medium contains (**a**) 1.1 mg/L and (**b**) 5 mg/L of elemental Fe. Yeast grown at 20 °C. 1—1–2 mg of $FeCl_3 \cdot 6H_2O$, 2—1–2 mg of $FeSO_4 \cdot 7H_2O$, 3—5 µL of 10 mg/L $FeCl_3 \cdot 6H_2O$ solution applied 2 h after inoculation.
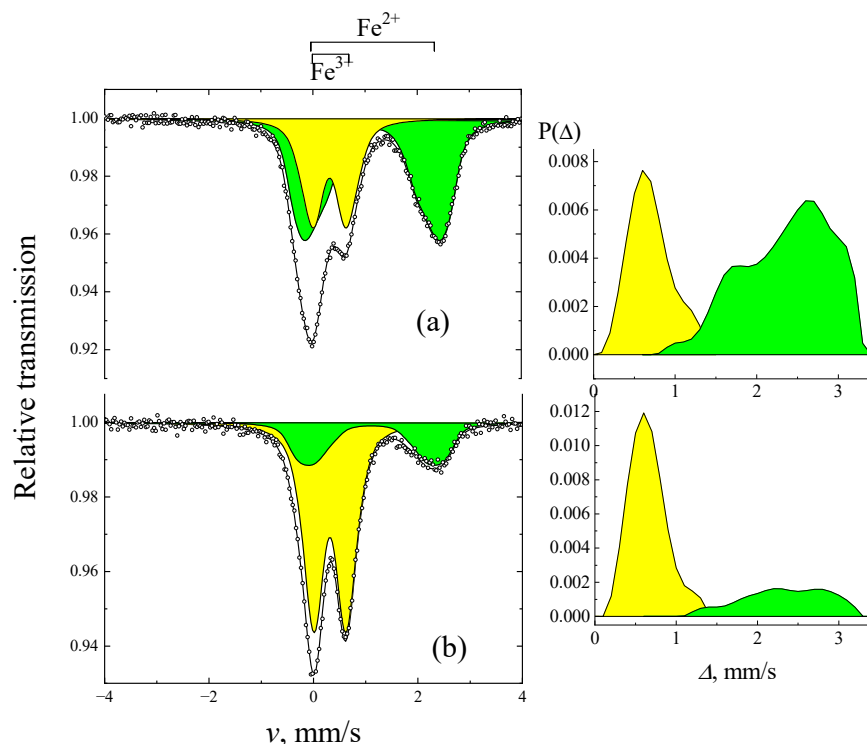
Figure 3. Mössbauer spectra of dried yeast growth media with applied $FeSO_4 \cdot 7H_2O$ (**a**) and $FeCl_3 \cdot 6H_2O$ (**b**) kept for 5 days. Right: quadrupole splitting distribution. Yellow is Fe^{3+} and green is Fe^{2+}.

Table 1. The parameters of Mössbauer spectra of ferric chloride $FeCl_3 \cdot 6H_2O$ and ferrous sulfate $FeSO_4 \cdot 7H_2O$ applied to growth media: *I*—relative intensity; δ—isomer shift; Δ—mean quadrupole splitting of distribution or quadrupole splitting of separate doublets.

| Sample	*I*, %	δ, mm/s	Δ, mm/s	
$FeSO_4 \cdot 7H_2O$	35 (34 ± 1) *	0.427 ± 0.004	0.695 (0.66 ± 0.01)	Fe^{3+}
	65 (35 ± 1; 31 ± 1)	1.245 ± 0.004	2.36 (1.97 ± 0.02; 2.75 ± 0.01)	Fe^{2+}
$FeCl_3 \cdot 6H_2O$	74 (73 ± 1)	0.423 ± 0.002	0.656 (0.63 ± 0.01)	Fe^{3+}
	26 (27 ± 1)	1.215 ± 0.010	2.33 (2.44 ± 0.02)	Fe^{2+}

* in parenthesis: data for separate doublets.

In order to exclude the influence of other compounds which are present in growth media, only ferric chloride $FeCl_3 \cdot 6H_2O$ and sugars were mixed. In the experiments with $FeCl_3 \cdot 6H_2O$ and sugars, immediately after mixing $FeCl_3 \cdot 6H_2O$ (hexahydrate ferric chloride) and fructose (or sucrose), the mixture became wet. After that, sugar dissolved in the released water and a viscous mass was formed. Accordingly, the Mössbauer spectrum of $FeCl_3 \cdot 6H_2O$, which is a characteristic asymmetric doublet with its isomer shift $\delta = 0.41 \pm 0.01$ mm/s and quadrupole splitting $\Delta = 0.94 \pm 0.01$ mm/s (Figure 4a) [34], transformed to a symmetric low-intensity doublet (Figure 4b). However, the valence state according to the isomer shift $\delta = 0.40 \pm 0.03$ mm/s and quadrupole splitting $\Delta = 0.60 \pm 0.06$ mm/s of doublet still remained Fe^{3+}.

After drying slightly above ambient temperature ($\approx$30 °C) for about a day or more, the mixture of $FeCl_3 \cdot 6H_2O$ and fructose turned more or less black (Figure 5a,b). In the case of the mixture on plastic tape a doublet attributed to Fe^{2+} (26–68% of the total spectral area depending on the conditions, Table 2) appeared in the Mössbauer spectrum (Figure 4c). The isomer shift $\delta = 1.12$–1.3 mm/s and quadrupole splitting of the doublet $\Delta = 2.2$–2.8 mm/s indicate ferrous chloride $FeCl_2 \cdot nH_2O$. For comparison, the contribution of Fe^{2+} was only

12% of the total spectral area when mixing ferric sulfate $Fe_2(SO_4)_3 \cdot H_2O$ and fructose, even after 6 days (Table 2).
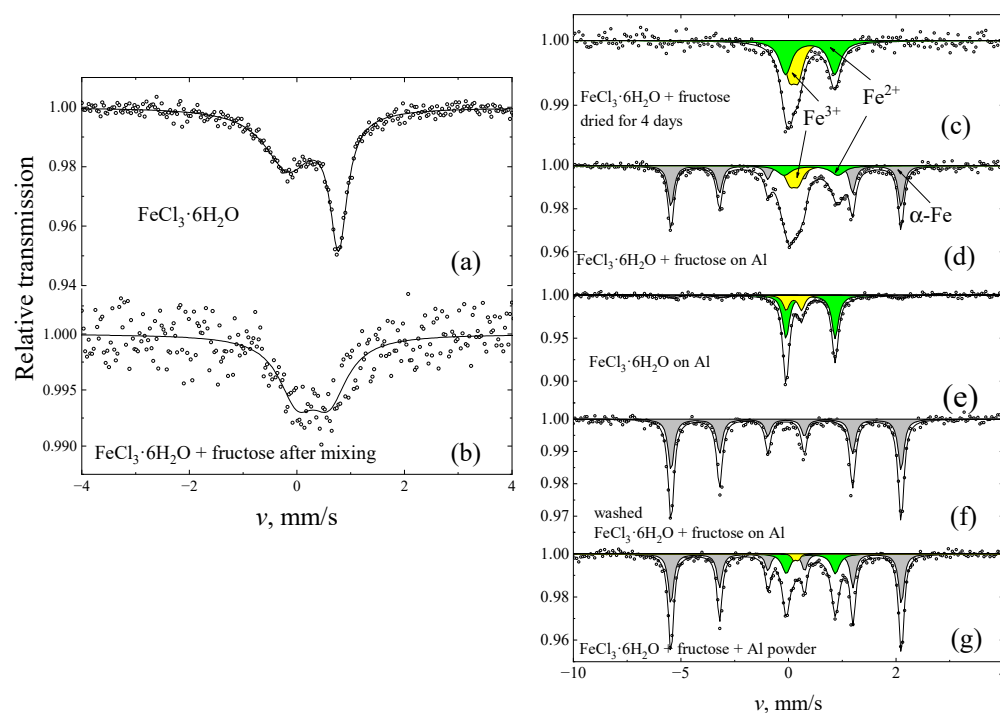
Figure 4. Mössbauer spectra of $FeCl_3 \cdot 6H_2O$ (**a**), mixture of $FeCl_3 \cdot 6H_2O$ with fructose before (**b**) and after drying on plastic tape for 4 days (**c**), dried mixture of $FeCl_3 \cdot 6H_2O$ with fructose on Al foil (**d**), $FeCl_3 \cdot 6H_2O$ on Al foil (**e**), Al foil when mixture of $FeCl_3 \cdot 6H_2O$ with fructose was washed out (**f**), and dried mixture of $FeCl_3 \cdot 6H_2O$ with fructose and Al powder on paper (**g**). Grey subspectrum is for α-Fe, yellow is Fe^{3+} and green is Fe^{2+}.
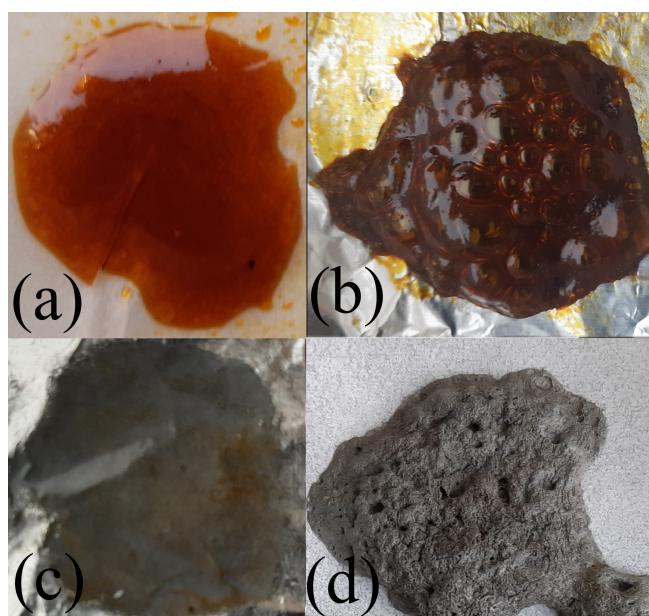
Figure 5. Mixture of $FeCl_3 \cdot 6H_2O$ with fructose on plastic tape (**a**) and Al foil (**b**), dried for 1 day at $\approx 30\ °C$, the aluminum foil with mixture washed out (**c**), mixture of $FeCl_3 \cdot 6H_2O$ with fructose and Al powder (**d**).

Table 2. The parameters of Mössbauer spectra of experiments with mixtures of ferric chloride $FeCl_3 \cdot 6H_2O$ and sugars: I—relative intensity; Γ—linewidth; δ—isomer shift; Δ—quadrupole splitting; B—hyperfine field.

| Sample	I, %	Γ, mm/s	δ, mm/s	Δ, mm/s	B, T	
$FeCl_3 \cdot 6H_2O$	100	1.07 ± 0.05 *	0.41 ± 0.01	0.94 ± 0.01		Fe^{3+}
FeClFP0d (1:1)	100	0.83 ± 0.05	0.40 ± 0.03	0.60 ± 0.06		Fe^{3+}
FeClFP1–2d (1:1)	74 ± 2	0.55 ± 0.02	0.37 ± 0.13	0.40 ± 0.01		Fe^{3+}
	26 ± 2	0.91 ± 0.09	1.14 ± 0.04	2.39 ± 0.07		Fe^{2+}
FeClFP1d (2:1)	32 ± 1	0.50 ± 0.04	0.36 ± 0.01	0.41 ± 0.02		Fe^{3+}
	68 ± 1	0.28 ± 0.01	1.17 ± 0.01	2.35 ± 0.01		Fe^{2+}
FeClFP4d (1:1)	41 ± 2	0.57 ± 0.09	0.37 **	0.40 ± 0.04		Fe^{3+}
	59 ± 3	0.67 ± 0.09	1.11 ± 0.02	2.28 ± 0.04		Fe^{2+}
FeClFAl1d (1:1)	24 ± 1	0.53 ± 0.04	0.37 **	0.37 ± 0.02		Fe^{3+}
	29 ± 1	0.76 ± 0.04	1.16 ± 0.01	2.49 ± 0.03		Fe^{2+}
	47 ± 1	0.33 ± 0.01	0.00 ± 0.01	0.00 ± 0.01	33.17 ± 0.02	Fe^{0}
After washing FeClFAl1d	100	0.33 ± 0.02	0.00 ± 0.01	−0.01 ± 0.01	33.23 ± 0.03	Fe^{0}
$FeCl_3 \cdot 6H_2O$ on Al	20 ± 1	0.33 ± 0.03	0.36 ± 0.05	0.71 ± 0.11		Fe^{3+}
	70 ± 2	0.36 ± 0.01	1.14 ± 0.02	2.28 ± 0.04		Fe^{2+}
	10 ± 2	0.34 ± 0.02	0.00 ± 0.06	0.00 **	33.7 ± 0.4	Fe^{0}
FeClFAlp1d (1:1:1)	2 ± 1	0.20 ± 0.09	0.46 ± 0.04	0.22 ± 0.05		Fe^{3+}
	30 ± 1	0.45 ± 0.01	1.15 ± 0.01	2.28 ± 0.01		Fe^{2+}
	68 ± 1	0.30 ± 0.01	0.01 ± 0.01	0.01 ± 0.01	33.2 ± 0.01	Fe^{0}
Washed FeClFAlp1d	19 ± 2	0.6 ± 0.2	0.29 ± 0.05	0.69 ± 0.09		Fe^{3+}
	81 ± 2	0.35 ± 0.01	0.00 ± 0.01	0.00 ± 0.01	33.18 ± 0.04	Fe^{0}
FeSFP6d (1:1)	88 ± 1	0.33 ± 0.01	0.42 ± 0.01	0.15 ± 0.01		Fe^{3+}
	12 ± 1	0.78 ± 0.09	1.24 ± 0.06	2.57 ± 0.08		Fe^{2+}

* lines area ratio 0.79 ± 0.05; linewidth ratio 0.36 ± 0.02; ** fixed.

When the mixture of $FeCl_3 \cdot 6H_2O$ and fructose was placed on aluminum foil gas bubbles formed inside the viscous black mass (Figure 5b). In the case when the mixture was on Al foil, in addition to Fe^{3+} and Fe^{2+} doublets, a sextet with parameters characteristic of α-Fe appeared (Figure 4d). The dependence on the surface on which the mixture was placed indicates that the mixture reacts with the aluminum foil. The reaction of pure $FeCl_3 \cdot 6H_2O$ with aluminum is characterized by strong corroding of aluminum foil, which damages its integrity. In this case, Fe^{2+} chloride is the dominant reaction product, while the α-Fe sextet is barely noticeable in the Mössbauer spectrum (Figure 4e).

In the Mössbauer spectrum of a mixture of $FeCl_3 \cdot 6H_2O$ and fructose on aluminum foil (Figure 4d), the sextet attributed to metallic iron is the most intense subspectrum (47% of the total area), while the Fe^{3+} and Fe^{2+} doublets account for 24 and 29% of the total area, respectively. After washing off the mixture from the aluminum surface, most of the metallic iron remains as a film on the Al foil, as shown in Figure 5c, and only the α-Fe sextet is visible in the spectrum (Figure 4f).

Metallic iron can also form on the surface of aluminum powder. Aluminum powder was added to the mixture of $FeCl_3 \cdot 6H_2O$ and fructose (mass ratio 1:1:1) (Figure 5d). In this case, the contribution of the α-Fe sextet increased to 68% of the total spectral area (Figure 4g). The magnetization data (Figure 6) confirm the formation of ferromagnetic α-Fe. The saturation magnetization $m_s \approx 7.5$ emu/g is obtained when extrapolating magnetization dependence of the mixture, $m = m_s - \text{const}/H$, with $H \rightarrow \infty$. The coercivity of ≈ 110 Oe was determined for this sample.
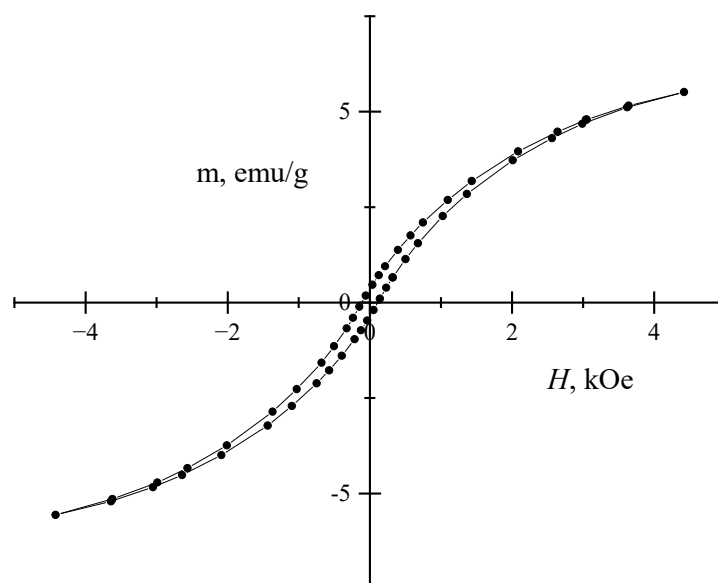
Figure 6. Magnetization dependence of mixture of $FeCl_3 \cdot 6H_2O$, fructose and aluminum powder on applied magnetic field.

3. Discussion

The inhibitory activity of two iron compounds shown in Figures 1 and 2 can be explained on the basis of detailed antimicrobial studies of ferric chloride and ferrous sulfate against pathogenic bacteria. The high bactericidal efficacy of ferric chloride against drug-resistant *Pseudomonas aeruginosa* has been linked to an increase in intracellular Fe^{2+} and the induction of ferroptosis via the Fenton reaction [28]. Cell lysis was observed at high concentrations. The antimicrobial mechanism of ferrous sulfate against *Staphylococcus aureus* was similar [29]. Ferric chloride was more effective than ferrous sulfate against *Pseudomonas aeruginosa* [28]. This can be explained by the existence of different Fe^{2+} and Fe^{3+} assimilation systems in *P. aeruginosa* cells. Since the growth inhibition of *S. cerevisiae* and *Metschnikowia* yeasts is greater in the case of ferrous sulfate $FeSO_4 \cdot 7H_2O$ than ferric chloride $FeCl_3 \cdot 6H_2O$, the mechanism of inhibition may be related more to a higher concentration of Fe^{2+} in the growth medium than to total excess of iron [5,6].

In the cases observed in Figures 1 and 2, iron in much larger quantities (of Fe^{2+} and Fe^{3+}) than the yeast cells need comes to yeast biomass from the growth medium. However, due to the production of pulcherrimin, the species of yeast belonging to the *Metschnikowia* clade can lower the concentration of free iron, binding it either outside the biomass or accumulating it in the form of red pigment—pulcherrimin—in the specialized cells—chlamydospores [3]. In this way, the initial toxic effect of iron on the yeast cells can be neutralized.

As the use of *Metschnikowia* yeast for fruit and berry protection is under investigation [11], the application of ferric chloride in combination with pulcherrimin-synthesizing yeast may be beneficial for stronger initial and long-lasting subsequent antimicrobial effects. That is, iron compounds can perform an initial biocidal function, after which the effects of iron compounds disappear as they dissipate, turn into insoluble hydroxides or pulcherrimin in the case of application of *Metschnikowia* spp., without having negative effects on plants or other living tissues. As antimicrobial substances, such iron compounds are suitable because they are biocompatible [28,29], and their effects disappear after performing the antimicrobial function.

The natural *Metschnikowia* spp. yeast environment, fruits and berries [12], is characterized by a high fructose content. The reducing properties of the sugar-containing medium (Figure 3b) may increase the antimicrobial effect of ferric chloride. This suggests that

the reducing properties of the medium should be taken into account when studying the antimicrobial effects of iron compounds.

Much more brown precipitates were observed in the places where ferric chloride $FeCl_3 \cdot 6H_2O$ was applied compared to ferrous sulphate $FeSO_4 \cdot 7H_2O$ (Figures 1 and 2a). The precipitation of Fe^{3+} can occur through hydrolysis and complexation reactions [35–38]. For example, due to Fe^{2+} oxidation and the formation of hydroxides, the concentration of free iron is very low in mildly acidic or alkaline natural waters [35]. Fe^{3+} hydrolysis and the formation of complexes will depend on the pH of the medium, its composition and other properties. A non-buffered growth medium with 5–6 pH was used in the study. It should be noted that hydroxide precipitates of Fe^{3+} can form at pH > 4 [35,36]. The amounts of ferric chloride $FeCl_3 \cdot 6H_2O$ and ferrous sulfate $FeSO_4 \cdot 7H_2O$ (1–2 mg) applied can change pH only locally and for a short time since there was no change in the characteristics of the agar growth medium (liquefaction of agar medium would be visible at pH < 3–4). The precipitates here are probably visible because of the high local concentration of Fe^{3+}.

Because of the low concentrations of free iron at biological pH, microorganisms have developed the ability to secrete special compounds of high affinity to iron—siderophores—to acquire iron from an insoluble form [39]. *Metschnikowia* spp. yeast secretes pulcherriminic acid, which is similar to siderophores but has another function—to reduce the availability of iron—which may be useful in preventing oxidative stress and restricting the Fenton reaction [18]. At the relatively high elemental iron concentration of 80 mg/L in the growth medium (when ferric chloride is distributed over the entire volume of the medium before its solidification and yeast inoculation), the accumulation of more than half of the total iron content in the yeast biomass is observed, mainly in the red pigment—pulcherrimin [3]. At the same time, such accumulation indicates the relative mobility of iron in the agar growth media. The movement of iron can be facilitated by iron reduction to Fe^{2+}, the formation of unstable complexes [40] and the secretion of compounds of the siderophore type.

A high ability of sugars to reduce ferric chloride was observed in the yeast growth medium and in the mixtures of ferric chloride ($FeCl_3 \cdot 6H_2O$) with sugars (Figures 3b and 4c, Tables 1 and 2). The occurrence of Fe^{2+} in the growth medium after supplementing the medium with ferric chloride is consistent with previous observations [3]. About 30% of iron in the form of Fe^{2+} was observed in *M. shanxiensis* M10 strain yeast biomass after 22 h of yeast growth with ≈5 mg/L of Fe in the growth medium. However, after another 22 h, the relative amount of Fe^{2+} decreased several times. The time dependence of the Fe^{2+} concentration can probably be attributed to the depletion of nutrients, including sugars, when yeast is present, so divalent iron may be more abundant in the initial yeast growth phase.

Due to the specificity of Mössbauer spectroscopy, a good spectral recording efficiency is achieved only for solids, so the samples were dried. The decrease in absorption area (Table 2) shortly after mixing ferric chloride ($FeCl_3 \cdot 6H_2O$) with fructose can be explained by the wetness of the mixture. It can be concluded that, first of all, mixing ferric chloride hexahydrate $FeCl_3 \cdot 6H_2O$ with fructose (the same as sugar) breaks down the crystalline structure and partially releases crystalline water.

In the mixture of $FeCl_3 \cdot 6H_2O$ and fructose, the isomeric shift δ = 1.12–1.3 mm/s and quadrupole splitting of the doublet Δ = 2.2–2.8 mm/s indicate the chemical state of Fe^{2+} corresponding to ferrous chloride $FeCl_2 \cdot nH_2O$. The variation in the quadrupole splitting could be due to the different amount of water in the $FeCl_2 \cdot nH_2O$ formula, where $n < 4$ [41]. In the case of yeast growth media, there are more opportunities for the formation of various iron compounds, so it is difficult to draw the same conclusion, even though the Mössbauer parameters are similar to those obtained for the mixtures.

It can also be assumed that iron complexes with fructose are not formed in the mixtures of fructose and $FeCl_3 \cdot 6H_2O$ because the quadrupole splitting of the ferric fructose complexes, Δ = 0.895 mm/s [8], is much larger than that of the observed Fe^{3+} doublet: Δ = 0.37–0.41 mm/s (Table 2). It should be noted that iron complexes with fructose have been observed in distilled water or methanol solutions [8,42]. In this study, water in mix-

tures is released from $FeCl_3 \cdot 6H_2O$ when it is mixed with fructose. However, the Fe^{3+} doublet in the Mössbauer spectra of the growth medium with ferrous sulfate $FeSO_4 \cdot 7H_2O$ and ferric chloride $FeCl_3 \cdot 6H_2O$ is broader and its lines are wider (Figure 3, Table 1), so the formation of Fe^{3+} complexes with fructose in the growth medium cannot be ruled out.

Although the reaction in mixtures of ferric chloride $FeCl_3 \cdot 6H_2O$ and fructose occurs near ambient temperature, the oxidizing power of ferric chloride increases with increasing ferric chloride concentration when oxidizing glucose with ferric chloride to obtain gluconic acid [25]. The release of gas (gas bubbles in the viscous mass of the mixture) is observed only when the mixture is placed on aluminum or the mixture contains aluminum powder (Figure 5b,d). As ferric chloride can remove the surface oxide layer on aluminum, the reaction of water with aluminum is possible [43]:

$$3H_2O + Al = Al(OH)_3 + 1.5H_2. \tag{1}$$
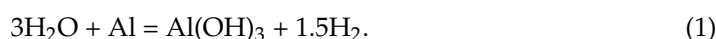
When placing pure ferric chloride $FeCl_3 \cdot 6H_2O$ on aluminum foil, the Mössbauer results (20% Fe^{3+}, 70% Fe^{2+} and 10% Fe^0 according to Table 1) generally correspond to the reaction of etching [20]

$$3FeCl_3 + Al = 3FeCl_2 + AlCl_3. \tag{2}$$
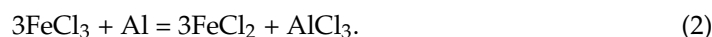
However, this reaction does not explain the formation of metallic iron when placing the mixture of $FeCl_3 \cdot 6H_2O$ and fructose on aluminum. The hydrogen formed in reaction (1) can participate in the reduction of ferrous chloride to metallic iron [1]:

$$FeCl_2 + H_2 = Fe + 2HCl. \tag{3}$$

Moreover, the following reactions were considered to occur in iron–aluminum chloride melts [32]:

$$FeCl_3 + Al = AlCl_3 + Fe, \tag{4}$$

$$3FeCl_2 + 2Al = 2AlCl_3 + 3Fe, \tag{5}$$

$$2FeCl_3 + Fe = 3FeCl_2, \tag{6}$$
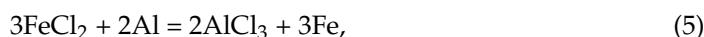
of which the first two were responsible for the formation of metallic iron. However, reactions (4) and (5) occurred efficiently at much higher than room temperature. In the mixtures of $FeCl_3 \cdot 6H_2O$ with fructose and aluminum, the reduction to metallic iron should occur mainly due to reactions (3) and (5), while the efficiency of the reverse reaction, (6), should decrease at the Al and Fe surfaces because the amount of ferric chloride ($FeCl_3$) decreases as it reacts with fructose and aluminum. This is shown by the experimental data, where the amount of Fe^{3+} is less than that of Fe^{2+} (Table 2). Furthermore, the interaction of Fe^{3+} with Fe^0 is hindered by the viscous medium which also traps hydrogen.

In the case of a mixture with Al, more Fe^{3+} is converted to metallic iron due to the larger surface area of the Al powder. Magnetization of 7.5 emu/g (Figure 6) corresponds to a 3.4% weight fraction of metallic iron in the sample when Fe^{3+} initially makes up about 6.6% of the sample mass. This is more or less consistent with the Mössbauer data (68% of Fe^0, Table 2). It is assumed that metallic iron is deposited as a thin film on the surface of the Al powder, so the surface plane of the film is, on average, oriented equally in all directions. The saturation of the magnetization of the sample with increasing magnetic field strength is achieved relatively slowly, because it is more difficult to magnetize the film when the direction of magnetization deviates from the plane of the film. The coercivity of $\approx$110 Oe is probably due to shape anisotropy, which depends on the thickness and structure of the Fe film [44].

4. Materials and Methods

Ferric chloride hexahydrate $FeCl_3 \cdot 6H_2O$ (Reachem Slovakia, Bratislava, Slovakia, 99% or Fluka Chemie GmbH, Buchs, Switzerland, 97%), ferrous sulfate heptahydrate $FeSO_4 \cdot 7H_2O$ (Carl Roth GmbH, Karlsruhe, Germany, 99.5%), ferric sulfate hydrate

$Fe_2(SO_4)_3 \cdot H_2O$ (Reachem Slovakia, Bratislava, Slovakia, 99%) and aluminum powder (Sigma-Aldrich, Steinheim, Germany, 99%, <75 μm) were used in this study. Fructose, sucrose and aluminum foil were bought at a regular store.

For yeast growth, non-buffered MR growth medium (pH 5–6) was applied. MR growth medium was prepared from 1% peptone (mycological, Liofilchem, Roseto, Italy) or 2% peptone M66 universal (Merck, Darmstadt, Germany or Sigma-Aldrich, Steinheim, Germany), 1% yeast extract (Liofilchem, Roseto, Italy), 2% glucose (Oriola, Espoo, Finland or Liofilchem, Roseto, Italy) and 2% agar (Difco Laboratories, Detroit, MI, USA). According to previous studies, the growth media contain 1.1 mg/L or 5 mg/L of elemental Fe. Small crystals (≈1–2 mg) of $FeSO_4 \cdot 7H_2O$ and $FeCl_3 \cdot 6H_2O$ or droplets (5 μL) of a 10 mg/L ferric chloride solution were applied directly to yeast streaks, spots or lawn grown in Petri dishes 2 h after yeast inoculation. *Metschnikowia* clade yeasts—*Metschnikowia sinensis* (strains—M4 and M6), *M. shanxiensis* (M10), *M. pulcherrima* (MP) [3,4], *Saccharomyces cerevisiae* haploid strain $\alpha'1$ and diploid strain Rom 100—were used to show the antimicrobial effects of iron compounds. *Metschnikowia* strains were isolated from spontaneous fermentations and identified as described before [3,12]. *Saccharomyces cerevisiae* Rom 100, the strain used in winemaking, and $\alpha'1$, the strain widely used in genetic research, were taken from the collection of the Institute of Botany (Nature Research Center, Vilnius, Lithuania). Yeast was inoculated after growth medium solidification and grown in the incubator at 20 °C. Experiments were repeated several times.

In the experiments with ferric chloride and sugars, $FeCl_3 \cdot 6H_2O$ and fructose or sucrose were mixed in a 1:1 (200 mg:200 mg) or 2:1 mass ratio (400 mg:200 mg) using a mortar and pestle. For comparison one sample of the mixture of ferric sulfate and fructose was made. The mixtures were placed on plastic tape or aluminum foil covering ≈ 4 cm^2 of area. Before recording the Mössbauer spectra, the mixtures were dried at approximately 30 °C for one or more days. In a further experiment, aluminum powder was added to the mixture of $FeCl_3 \cdot 6H_2O$ and fructose and placed on paper. Mixing with sucrose gives quite similar results to mixing with fructose; therefore, the results of experiments with sucrose are not presented here. Table 2 uses abbreviated sample names: FeClFP1d (1:1), FeClSAl2d (1:1), etc., where FeCl is ferric chloride; FeS is ferric sulfate $Fe_2(SO_4)_3 \cdot H_2O$; F is fructose; P is plastic tape; Al is aluminum foil; Alp—aluminum powder; nd—dried for *n* days; and (1:1)—components ratio.

Mössbauer spectra were measured using a $^{57}Co(Rh)$ source and Mössbauer spectrometer (Wissenschaftliche Elektronik GmbH, Starnberg, Germany). The quadrupole distributions or separate doublets and the sextet were used to fit to the Mössbauer spectra applying WinNormos Site and Dist, version 3.0 software. Isomer shifts are given relative to α-Fe. The changes in the valence state of iron $Fe^{3+} \rightarrow Fe^{2+} \rightarrow Fe^0$ were evaluated according to the parameters of the Mössbauer spectra. Since Fe^{3+}, Fe^{2+} and Fe^0 (metallic iron) states have a sufficiently different isomer shift δ, quadrupole splitting Δ and hyperfine field *B*, these states can be easily distinguished as shown in the Mössbauer spectra by different colors.

A vibrating sample magnetometer consisting of a lock-in amplifier SR510 (Stanford Research Systems, Sunnyvale, CA, USA), a Gauss-/Teslameter FH-54 (Magnet Physics, Cologne, Germany) and a laboratory magnet supplied by a power source SM 330-AR-22 (Delta Elektronika, Zierikzee, The Netherlands) were applied for magnetization measurements.

5. Conclusions

A significant reduction of Fe^{3+}, 26% in the yeast growth media with ferric chloride $FeCl_3 \cdot 6H_2O$, and iron, up to 68% in the $FeCl_3 \cdot 6H_2O$ and fructose mixtures, is observed. If the mixture of ferric chloride and fructose is placed on aluminum foil, a thin film of metallic iron is formed on its surface. In this case, fructose reduces ferric chloride to Fe^{2+}, traps hydrogen resulting from the reaction of aluminum with water and also protects the aluminum surface from significant corrosion. Ferrous sulfate $FeSO_4 \cdot 7H_2O$ significantly inhibited the growth of *Metschnikowia* and *S. cerevisiae* yeasts. In the case of ferric chloride, $FeCl_3 \cdot 6H_2O$, the zone of growth inhibition was smaller. Since the effect of reduced Fe^{3+} to

Fe^{2+} in growth media cannot be ruled out, it is generally concluded that the reducing ability of the medium may be important for the antimicrobial applications of iron compounds.

References

1. Luidold, S.; Antrekowitsch, H. Hydrogen as a Reducing Agent: State-of-the-Art Science and Technology. *JOM* **2007**, *59*, 20–26. [CrossRef]
2. Xing, Z.Y.; Lu, J.; Ji, X. A brief review of metallothermic reduction reactions for materials preparation. *Small Methods* **2018**, *2*, 1800062. [CrossRef]
3. Mažeika, K.; Šiliauskas, L.; Skridlaite, G.; Matelis, A.; Garjonytė, R.; Paškevicius, A.; Melvydas, V. Features of iron accumulation at high concentration in pulcherrimin-producing *Metschnikowia* biomass. *JBIC J. Biol. Inorg. Chem.* **2021**, *26*, 299–311. [CrossRef] [PubMed]
4. Melvydas, V.; Staneviciene, R.; Balynaite, A.; Vaiciuniene, J.; Garjonyte, R. Formation of self-organized periodic patterns around yeasts secreting a precursor of red pigment. *Microbiol. Res.* **2016**, *193*, 87–93. [CrossRef] [PubMed]
5. Winterbourn, C.C. Toxicity of iron and hydrogen peroxide: The Fenton reaction. *Toxicol. Lett.* **1995**, *82/83*, 969–974. [CrossRef] [PubMed]
6. Galaris, D.; Barbouti, A.; Pantopoulos, K. Iron homeostasis and oxidative stress: An intimate relationship. *BBA-Mol. Cell Res.* **2019**, *1866*, 118535. [CrossRef] [PubMed]
7. Christides, T.P.; Sharp, P. Sugars increase non-heme iron bioavailability in human epithelial intestinal and liver cells. *PLoS ONE* **2013**, *8*, e83031. [CrossRef] [PubMed]
8. Pulla Rao, C.; Geetha, K.; Raghava, M.S.S. Fe(III) complexes of D-glucose and D-fructose. *BioMetals* **1994**, *7*, 25–29.
9. Maicas, S.; Mateo, J.J. The Life of Saccharomyces and Non-Saccharomyces Yeasts in Drinking Wine. *Microorganisms* **2023**, *11*, 1178. [CrossRef] [PubMed]
10. Abeln, F.; Hicks, R.H.; Auta, H.; Moreno-Beltrán, M.; Longanesi, L.; Henk, D.A.; Chuck, C.J. Semi-continuous pilot-scale microbial oil production with *Metschnikowia pulcherrima* on starch hydrolysate. *Biotechnol. Biofuels* **2020**, *13*, 127. [CrossRef] [PubMed]
11. Freimoser, F.M.; Rueda-Mejia, M.P.; Tilocca, B.; Migheli, Q. Biocontrol yeasts: Mechanisms and applications. *World J. Microb. Biot.* **2019**, *35*, 154. [CrossRef] [PubMed]
12. Melvydas, V.; Svediene, J.; Skridlaite, G.; Vaiciuniene, J.; Garjonyte, R. In vitro inhibition of *Saccharomyces cerevisiae* growth by *Metschnikowia* spp. *triggered by fast removal of iron via two ways. Braz. J. Microbiol.* **2020**, *51*, 1953–1964. [CrossRef] [PubMed]
13. Commenges, A.; Lessard, M.-H.; Coucheney, F.; Labrie, S.; Drider, D. The biopreservative properties of *Metschnikowia pulcherrima* LMA 2038 and *Trichosporon asahii* LMA 810 in a model fresh cheese, are presented. *Food Biosci.* **2024**, *58*, 103458. [CrossRef]
14. Kregiel, D.; Czarnecka-Chrebelska, K.H.; Schusterová, H.; Vadkertiová, R.; Nowak, A. The *Metschnikowia pulcherrima* clade as a model for assessing inhibition of *Candida* spp. and the toxicity of its metabolite, pulcherrimin. *Molecules* **2023**, *28*, 5064. [CrossRef] [PubMed]
15. Pawlikowska, E.; James, S.A.; Breierova, E.; Kregiel, H.A.D. Biocontrol capability of local *Metschnikowia* sp. isolates. *Antonie Van Leeuwenhoek J. Microb.* **2019**, *112*, 1425–1445. [CrossRef] [PubMed]
16. Sipiczki, M. *Metschnikowia pulcherrima* and related pulcherrimin-producing yeasts: Fuzzy species boundaries and complex antimicrobial antagonism. *Microorganisms* **2020**, *8*, 1029. [CrossRef] [PubMed]
17. MacDonald, C. The structure of pulcherriminic acid. *Can. J. Chem.* **1963**, *41*, 165–172. [CrossRef]
18. Charron-Lamoureux, V.; Haroune, L.; Pomerleau, M.; Hall, L.; Orban, F.; Leroux, J.; Rizzi, A.; Bourassa, J.-S.; Fontaine, N.; d'Astous, É.V.; et al. Pulcherriminic acid modulates iron availability and protects against oxidative stress during microbial interactions. *Nat. Commun.* **2023**, *14*, 2536. [CrossRef] [PubMed]
19. Zhike, W.; Jianting, C.; Cunling, Y. Application of ferric chloride both as oxidant and complexant to enhance the dissolution of metallic copper. *Hydrometallurgy* **2010**, *105*, 69–74. [CrossRef]
20. Cakır, O. Chemical etching of aluminium. *J. Mater. Process. Technol.* **2008**, *199*, 337–340. [CrossRef]
21. Ogura, Y.; Kobayashi, C.; Ooba, Y.; Yahata, N.; Sakamoto, H. Low temperature deposition of metal films by metal chloride reduction chemical vapor deposition. *Surf. Coat. Technol.* **2006**, *200*, 3347–3350. [CrossRef]
22. Lee, C.S.; Robinson, J.; Chonga, M.F. A review on application of flocculants in wastewater treatment. *Process Saf. Environ.* **2014**, *92*, 489–508. [CrossRef]
23. So, R.C.; Carreon-Asok, A.C. Molecular design, synthetic strategies, and applications of cationic polythiophenes. *Chem. Rev.* **2019**, *119*, 11442–11509. [CrossRef] [PubMed]

24. Li, L.; Sun, J.; Cai, C.; Wang, S.; Pei, H.; Zhang, J. Corn stover pretreatment by inorganic salts and its effects on hemicellulose and cellulose degradation. *Bioresour. Technol.* **2009**, *100*, 5865–5871. [CrossRef] [PubMed]

25. Zhang, H.; Li, N.; Pan, X.; Wu, S.; Xie, J. Oxidative conversion of glucose to gluconic acid by iron(III) chloride in water under mild conditions. *Green Chem.* **2016**, *18*, 2308–2312. [CrossRef]

26. Žalneravičius, R.; Paškevičius, A.; Kurtinaitiene, M.; Jagminas, A. Size-dependent antimicrobial properties of the cobalt ferrite nanoparticles. *J. Nanopart. Res.* **2016**, *18*, 300. [CrossRef]

27. Sun, H.-Q.; Lu, X.-M.; Gao, P.-J. The exploration of the antibacterial mechanism of Fe^{3+} against bacteria. *Braz. J. Microb.* **2011**, *42*, 410–414. [CrossRef]

28. Huang, M.; Wang, Z.; Yao, L.; Zhang, L.; Gou, X.; Mo, H.; Li, H.; Hu, L.; Zhou, X. Ferric chloride induces ferroptosis in *Pseudomonas aeruginosa* and heals wound infection in a mouse model. *Int. J. Antimicrob. Agents* **2023**, *61*, 106794. [CrossRef]

29. Zhen, W.; Lia, H.; Zhou, W.; Lee, J.; Liu, Z.; An, Z.; Xu, D.; Mo, H.; Hu, L.; Zhou, X. Ferrous sulfate-loaded hydrogel cures *Staphylococcus aureus* infection via facilitating a ferroptosis-like bacterial cell death in a mouse keratitis model. *Biomaterials* **2022**, *290*, 121842. [CrossRef]

30. Karathia, H.; Vilaprinyo, E.; Sorribas, A.; Alves, R. Saccharomyces cerevisiae as a model organism: A comparative study. *PLoS ONE* **2011**, *6*, e16015. [CrossRef] [PubMed]

31. Duina, A.A.; Miller, M.E.; Keeney, J.B. Budding yeast for budding geneticists: A primer on the *Saccharomyces cerevisiae* model system. *Genetics* **2014**, *197*, 33–48. [CrossRef] [PubMed]

32. Foley, E.; Moyle, F.J. The reduction of ferric chloride by aluminium in aluminium chloride melts. *J. Appl. Chem. Biotechnol.* **1972**, *22*, 867–875. [CrossRef]

33. Melvydas, V.; Mazeika, K.; Matelis, A.; Paskevicius, A.; Garjonyte, R. Response of pulcherrimin-producing Metschnikowia yeast to solid iron-containing materials: In vitro and in vivo studies. *Mycologia*, (submitted, under review).

34. Thrane, N.; Trumpy, G. Spin-spin relaxation and Karyagin-Gol'danskii effect in $FeCl_3$ $6H_2O$. *Phys. Rev. B* **1970**, *1*, 153–155. [CrossRef]

35. Stefansson, A. Iron(III) hydrolysis and solubility at 25 °C. *Environ. Sci. Technol.* **2007**, *41*, 6117–6123. [CrossRef] [PubMed]

36. Irto, A.; Cigala, R.M.; De Stefano, C.; Crea, F. Advances in iron(III) hydrolysis studies. Effect of the metal concentration, ionic medium and ionic strength. *J. Mol. Liq.* **2023**, *1*, 123361. [CrossRef]

37. Millero, F.J.; Yao, W.; Aicher, J. The speciation of Fe(II) and Fe(III) in natural waters. *Mar. Chem.* **1995**, *50*, 21–39. [CrossRef]

38. Cotton, S.A. Iron(III) chloride and its coordination chemistry. *J. Coord. Chem.* **2018**, *71*, 3415–3443. [CrossRef]

39. Neilands, J.B. Methodology of siderophores. In *Siderophores from Microorganisms and Plants*; Clarke, M.J., Goodenough, J.B., Ibers, J.A., Jorgensen, C.K., Mingos, D.M.P., Neilands, J.B., Palmer, G.A., Reinen, D., Sadler, P.J., Weiss, R., Eds.; Springer: Berlin, Germany, 1984; pp. 1–25.

40. Murphy, J.M.; Powell, B.A.; Brumaghim, J.L. Stability constants of bio-relevant, redox-active metals with amino acids: The challenges of weakly binding ligands. *Coord. Chem. Rev.* **2020**, *412*, 212253. [CrossRef]

41. Bull, J.N.; Maclagan, R.G.A.R.; Fitchett, C.M.; Craighead Tennant, W. A new isomorph of ferrous chloride tetrahydrate: A ^{57}Fe Mossbauer and X-ray crystallography study. *J. Phys. Chem. Sol.* **2010**, *71*, 1746–1753. [CrossRef]

42. Charley, P.J.; Sarkar, B.; Stitt, C.F.; Saltman, P. Chelation of iron by sugars. *Biochim. Biophys. Acta* **1963**, *69*, 313–321. [CrossRef] [PubMed]

43. Kótai, L.; Lippart, J.; Gács, I. Deuterium isotope separation in the chemical reaction of aluminium amalgam and water. *Eur. Chem. Bull.* **2012**, *1*, 37–38. [CrossRef]

44. Mažeika, K.; Reklaitis, J.; Nicolenco, A.; Vainoris, M.; Tsyntsaru, N.; Cesiulis, H. Magnetic state instability of disordered electrodeposited nanogranular Fe films. *J. Magn. Magn. Mat.* **2021**, *540*, 168433. [CrossRef]